JOURNAL OF APPLIED ELECTROCHEMISTRY 21 (1991) 483–486

Morphologies of anodic oxide films deduced from dissolution studies

M. M. HEFNY

Department of Chemistry, Faculty of Science, U.A.E. University, Al-Ain, P.O. Box 17771, United Arab Emirates

Received 15 February 1990; revised 14 November 1990

Study of the chemical stripping of anodic oxide films on hafnium, zirconium, tungsten and aluminium has led to the deduction of the morphology of the respective oxides. Away from the boundary region hafnium oxide is a compact, smooth, homogenous and crystalline oxide. Zirconium oxide has a superficial disorder layer which constitutes about 17% of the entire film. Tungsten oxide deposits are composed of two defective partial layers the outer one being more disordered. Aluminium oxide is a porous film. A schematic representation of each film had been presented.

1. Introduction

Knowledge of the morphology of surfaces is important for the technical applications of solids [1]. It is possible to infer some of the surface features of solids by expensive techniques such as Auger and/or SEM [2]. Alternatively, it is possible to deduce some of the surface characteristics by etching techniques [3]. Previously, the capacitance (inverse thickness) technique was used successfully to reveal the profiles of defects in anodic oxide films [4]. These results are important for the elucidation of several phenomena in materials science such as corrosion rates [5], efficiency of the surface of a semiconductor in solar cell technology [6] and quality of electrodeposited layers [7].

Surface oxide films are usually composed of more than one layer. These layers may differ in their chemical composition, crystallinity or porosity. The differences may arise from: (i) the possibility of the presence of the metal ion in more than one oxidation state [8], (ii) change of the mechanism of growth of the oxide with thickness, e.g., from the solid state mechanism into dissolution/precipitation [9, 10] and (iii) increase of the internal compressive stresses with increase of the oxide thickness [11].

The aim of the present investigation is to reveal the morphology of some of the anodic oxide films from the previously established kinetic features of their chemical dissolution reactions [12, 15]. The methodology and techniques of measurements are essentially the same as those given previously [4, 16, 17].

2. Results and discussion

It has been found that the shape of the kinetic curve representing the selective dissolution of a given oxide depends on its nature, as shown in Figs 1–3, for hafnium, zirconium and tungsten oxides and Figs 4 and 5 for aluminium oxide, respectively.

Figure 1 shows the decrease of the reciprocal of the electrode capacitance, C_m^{-1}, which measures the thickness of the remaining anodic oxide film on hafnium with immersion time [12]. This figure indicates that hafnium oxide dissolves at a constant rate. This feature has been observed during the dissolution of the anodic oxide film on hafnium in several solutions such as HCl [12], H_2SO_4 [18] and NaOH [19] over wide ranges of concentration. Therefore one may conclude that, away from the boundary regions, this oxide is more or less homogenous (composed of one layer). This conclusion accords with the structure revealed by other techniques [11]; it is crystalline. Thus one may represent the structure of this oxide as shown in Fig. 6a. This figure shows the morphology of the anodic oxide film on hafnium regardless of the profile of atomic defects therein [4].

Dissolution of the anodic oxide film on zirconium may proceed in accordance with one or two rate laws, depending on the concentration of the dissolving solution, Fig. 2. This indicates that the anodic oxide film on zirconium is composed of two layers. The outer one is more reactive than the inner one, possibly due to a higher concentration of defects, difference in composition and/or lower degree of crystallinity. A schematic representation of the morphology of this film is given in Fig. 6b. Evidence for the suggested structure of the outer, as compared to the inner layer, is that it dissolves faster in the relatively concentrated solution since region B_1, Fig. 2, has a higher slope than region B_2. On the other hand, in the dilute sulphuric acid solutions sealing of the outer layer occurs (region B_1', Fig. 2). This is indicated by the increase in the overall thickness of the oxide (the reciprocal of capacitance) as the formation reaction overtakes the dissolution process. It is worth mentioning that defects act bifunctionally; they initiate both formation as well as dissolution of the oxide [20]. So, the behaviour of the anodic oxide film on zirconium can be visualized as follows; in the concentrated solution dissolution of the outer layer predominates

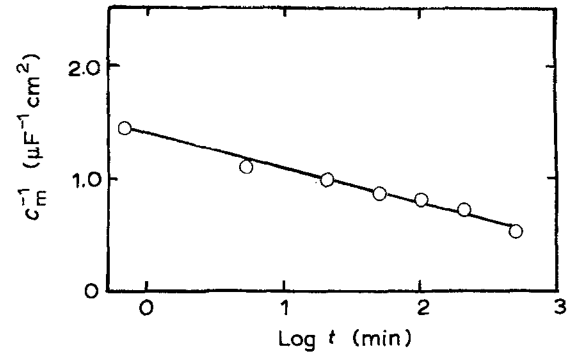

Fig. 1. Reciprocal capacitance against logarithm of the immersion time for the anodized hafnium electrode in 1.0 M HCl; the anodization voltage, current and solution concentration are 25 V, 2.5 mA cm^{-2} and 0.25 M H_2SO_4, respectively.

initially; however, at a later stage the thickness decreases rather slowly due to the slower dissolution of the less reactive inner layer (region B_2, Fig. 2). In the dilute solution, sealing of the outer layer occurs, which gives rise to a decrease in capacitance, C_m (increase of thickness) as revealed by the region B_1'. Fig. 2: a limiting thickness is eventually reached, region B_2' in Fig. 2.

It is worth noting that the extrapolation of region B_2' and B_1 intersect at zero time, Fig. 2. This confirms the fact that the process occurring during the early period of immersion of the oxide in 0.02 M H_2SO_4 (region B_1', Fig. 2) may be viewed as a repair or sealing phenomenon.

The relative thickness of the outer and inner layers of the oxide can be estimated from the capacitance values corresponding to the moment of immersion (0.46 μF cm^{-2}) and at the stage (30 min later) corresponding to complete dissolution of the outer layer (0.55 μF cm^{-2}). According to these values the outer layer constitutes 17% and the inner layer 83% of the entire film.

In almost all acid solutions the anodic oxide film on tungsten dissolves as shown in Fig. 3. This curve reveals that the film is composed of two layers, each susceptible to dissolution [14]. The outer layer dissolves faster since the slope of the region C_1 is higher than that of the region C_2, Fig. 3. Thus the structure of the anodic oxide film on tungsten can be represented in a duplex manner, the outer layer being the more defective, Fig. 6c.

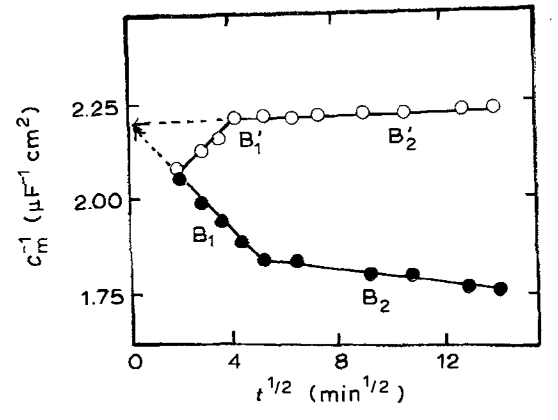

Fig. 2. Variation of the thickness of the oxide on the anodized zirconium electrode represented by the reciprocal of the electrode capacitance, C_m^{-1}, with the square root of the immersion time, $t^{1/2}$, at different sulphuric acid concentrations: (○) 0.02 and (●) 0.50 M. The anodization voltage, current and solution concentration are 25 V, 2.17 mA cm^{-2} and 0.50 M H_2SO_4, respectively.

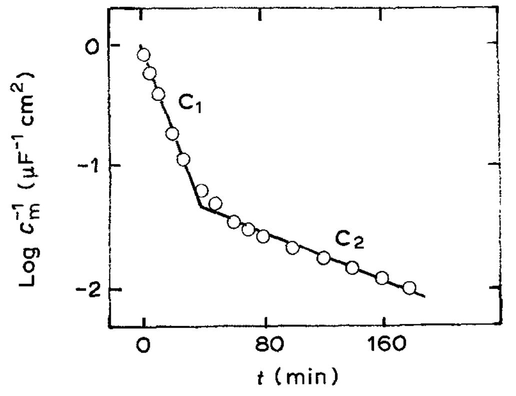

Fig. 3. Decrease of log C_m^{-1} with time during dissolution of the anodic oxide film on tungsten in 0.1 M HCl. The oxide was formed galvanostatically in 0.1 M HCl at a current density of 0.50 mA cm^{-2} up to a formation voltage of 20.0 V.

In the same manner as for zirconium the relative thickness of the outer and inner layers are 5% and 95%, respectively. These values should be considered cautiously from the quantitative point of view because the capacitance method for measuring the thickness becomes more accurate the more perfect the oxide [21]. The last condition is satisfied more for zirconium than for tungsten.

Dissolution of the anodic oxide film on aluminium follows the kinetic curve shown in Fig. 4; the corresponding potential decay curve is shown in Fig. 5. The striking feature in this case is that there is a period of time during which the thickness of the oxide decreases rather slowly (region d_1, Fig. 4 and region d_1, Fig. 5) and then the thickness decreases sharply (region d_2, Fig. 4 and region d_2 Fig. 5).

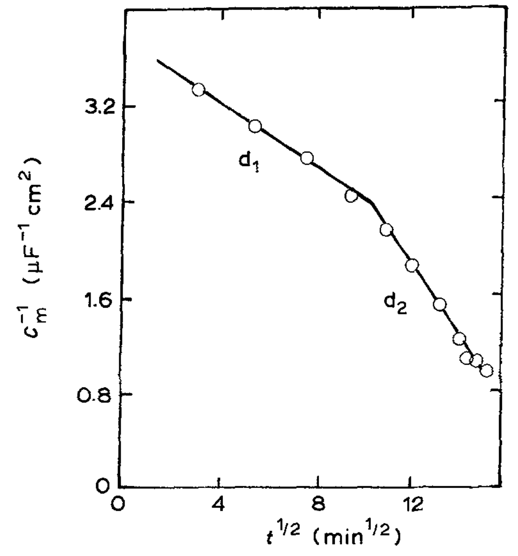

Fig. 4. Decrease of C_m^{-1} with the square root of the immersion time, $t^{1/2}$, of the anodic oxide film on aluminium in 0.25 M KF. The oxide was formed galvanostatically according to the following anodization condition; voltage, current and solution concentration are 60 V, 5.952 mA cm^{-2} and 1.0 M H_3PO_4, respectively.

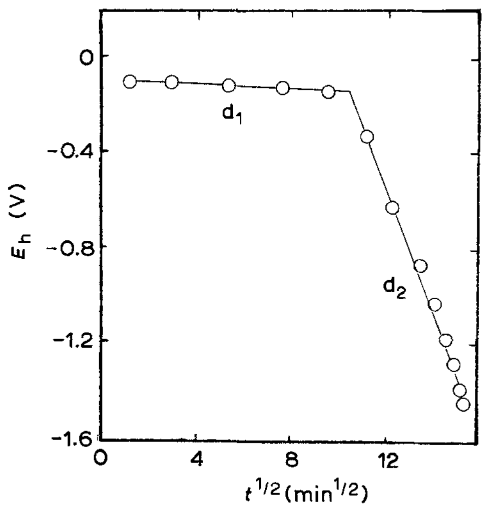

Fig. 5. Decay of the open circuit potential, E_h, against SHE of the anodized aluminium electrode during dissolution of the same oxide specified in the capture of Fig. 4.

Previous studies reveal that the results of open circuit potential measurements (Fig. 5), recorded simultaneously with those of the electrode capacitance (Fig. 4) during the stripping of the oxide, are in agreement with regard to the kinetics of the dissolution process [12, 22], i.e. under certain conditions the electrode potential [23, 24] and electrode capacitance [21] are proportional to the instantaneous thickness of the oxide.

The dissolution behaviour of the anodic oxide film on aluminum suggests that it has the morphology shown in Fig. 6d; it is composed mainly of a porous (outer) layer and a barrier (inner) layer. During the period of the region d_1. Fig. 4 (the region d_1, Fig. 5), the oxide dissolves by a pore widening mechanism [25], *i.e.*, the oxide dissolves while its thickness decreases insignificantly. At a critical time or thickness (pore depth to width ratio), infinite exposure of the oxide to the solution occurs which gives rise to an avalanche dissolution, hence a sharp increase in dissolution rate occurs, (region d_2 Fig. 4 or region d_2 Fig. 5). The incomplete parallelism between the results of potential, Fig. 5, and those of capacitance, Fig. 4, can be attributed to side reactions associated with the dissolution process, e.g., hydration of the porous layer [26]. These evidently change the electrical properties, of the inner and outer regions to different degrees and hence the measured potential and capacitance values are not exactly parallel. Capacitance and potential can respond to the properties of a given film to different degrees. For example with increasing insulating properties of an oxide capacitance becomes a more accurate index for measuring the oxide thickness while the open circuit potential ceases to change [18].

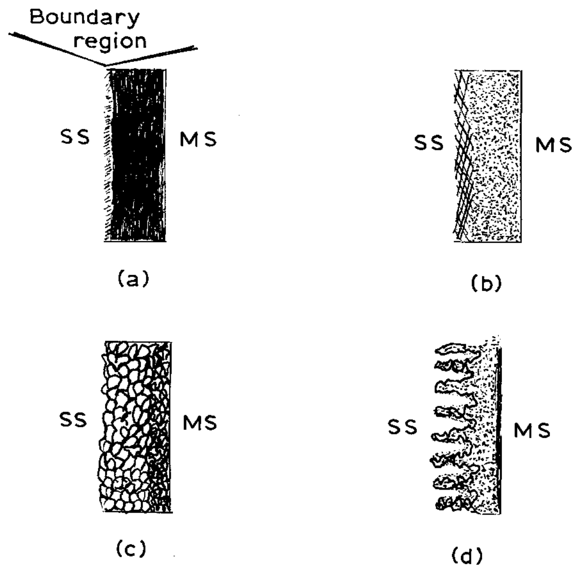

Fig. 6. Sketch of the likely morphology of the anodic oxide film on (a) hafnium, (b) zirconium, (c) tungsten and (d) aluminium. MS = metal side; SS = solution side.

3. Conclusion

The order of increasing complexity of the structures of the investigated anodic oxide films is as follows: hafnium oxide < zirconium oxide < tungsten oxide < aluminium oxide. (Aluminium oxide has the most complicated structure.) This order is almost the same for the ease of formation of atomic defects in the respective oxides [27]. This means that when there is a relatively large concentration of atomic disorders (say in tungsten oxide), the defects interact by disproportionation to give voids or even pores (e.g. in aluminium oxide). These reactions may occur consecutively to give rise to splitting of the film into two strata and, hence, different morphologies according to the nature of the oxide. Since the role of the nature of the oxide can be represented by the metal-oxygen bond energy in the oxide [4, 27], the deduced morphologies are thermodynamically justified.

References

[1] J. W. Schultz, *Mater. Chem. Phys.* **22** (1989) 417.
[2] R. Keim, *P. T. Procestech.* **44** (1989) 58.
[3] W. F. Tseng, H. Lessoff and R. Gorman, *J. Electrochem. Soc.* **132** (1985) 3067.
[4] M. M. Hefny, A. S. Mogoda and M. S. El-Basiouny, *Br. Corros. J.* **21** (1986) 109.
[5] B. Mazza, P. Pedeferri, D. Sinigaglia, A. Cigada, L. Lazzari, G. Re and D. Wenger, *J. Electrochem. Soc.* **123** (1976) 1157.
[6] T. Surek, C. B. Hari Rao, J. C. Swartz and L. C. Garone, *ibid.* **124** (1977) 112.
[7] W. Engelmaier and T. Kessler, *ibid.* **125** (1978) 36.
[8] H. C. Gatos (ed.), 'The surface chemistry of metals and semiconductors', Wiley, London (1965).
[9] A. Di Paola, F. D. Quarto and C. Sunseri, *Corros. Sci.* **20** (1980) 1067 and 1079.
[10] R. D. Armstrong, *Corros. Sci.* **11** (1971) 693.
[11] J. S. L. Leach and B. R. Pearson, *ibid.* **28** (1988) 43.
[12] M. M. Hefny, M. S. El-Basiouny, A. G. Gad Allah and S. A. Salih, *Electrochim. Acta* **28** (1983) 1811.
[13] M. S. El-Basiouny, A. A. Mazhar, F. El-Taib Heakal and M. A. Ameer, *J. Electroanal Chem.* **147** (1983) 181.
[14] M. M. Hefny, A. G. Gad Allah and A. S. Mogoda, *B. Electrochem.* **3** (1987) 11.
[15] W. A. Badawy, M. M. Ibrahim and M. S. El-Basiouny, *Corrosion* **42** (1986) 324.
[16] M. S. El-Basiouny, A. M. El-kot and M. M. Hefny, *Br. Corros. J.* **14** (1979) 51.
[17] A. G. Gad Allah, A. A. Mazhar, F. El-Taib Heakal and M. A. Ameer, *J. Appl. Electrochem.* **19** (1989) 213.
[18] M. S. El-Basiouny, A. M. Bekheet and M. M. Hefny, *Corrosion* **35** (1979) 566.

[19] A. G. Gad Allah, H. A. Abd El-Rahman and M. M. Abou-Romia, *J. Appl. Electrochem.* **18** (1988) 532.

[20] A. A. Mazhar, M. M. Hefny, F. El-Taib Heakal and M. S. El-Basiouny, *Br. Corros. J.* **18** (1983) 156.

[21] L. Young, 'Anodic Oxide Films', Academic Press, London (1961).

[22] M. M. Hefny, M. S. El-Basiouny and A. S. Mogoda, *Corrosion* **39** (1983) 266.

[23] A. K. Vijh, *Corros. Sci.* **12** (1972) 105.

[24] J. M. Abd El Kader, F. M. Abd El Wahab, H. A. El-Shayeb and G. A. Kheder, *Br. Corros. J.* **16** (1981) 11.

[25] M. Nagayama, K. Tamura and H. Takahashi, *Corros. Sci.* **12** (1972) 133.

[26] L. D. Burke and M. E. G. Lyons, in 'Modern aspects of electrochemistry', Vol. 18 (edited by R. A. White, J. O'M Bockris and B. E. Conway), Plenum, New York, (1986) ch. 4.

[27] A. K. Vijh, *J. Electrochem. Soc.* **116** (1969) 972.